MODIFICATION OF CANAL FLOW DUE TO STREAM-AQUIFER INTERACTION

By A. M. Wasantha Lal,[1] Member, ASCE

ABSTRACT: Unsteady canal flow in an integrated canal-flow–groundwater-flow system is analyzed by solving the coupled equations governing canal flow, groundwater flow and the seepage between them. Analytical solutions are obtained for the coupled system for small water-level disturbances using Fourier analysis methods and complex variables. Dimensionless parameter groups characterizing the aquifer, the canal, and the sediment layer are identified using the governing equations and the solution. The influence in the aquifer and the semipermeable bottom sediment layer due to disturbances in canal flow is studied. The analytical solutions are compared to numerical solutions obtained using the MODFLOW model and the Hydrologic Simulation Engine of the South Florida Regional Simulation Model. Results of the analysis are useful in determining the range of aquifer, sediment, and canal characteristics for which stream-aquifer interaction is important. The results can be used to determine the conditions for which the canal is hydraulically disconnected from the aquifer because of the sediment layer. The analytical solution is useful to understand the propagation characteristics of small-amplitude water-level disturbances in the canal and the aquifer. The characteristics studied include the amplitude decay constant and the speed. The solution can be used to design benchmark problems that can be used to evaluate integrated canal-flow–groundwater-flow models. The results of the study can be used to estimate the space and time steps needed in the canal and the aquifer when simulating stream-aquifer interaction.

INTRODUCTION

As part of the overall effort to restore the Everglades ecosystem in South Florida, and to meet its regional water management responsibilities, the South Florida Water Management District (SFWMD) (SFWMD 1999) and other organizations have developed a number of mathematical models to simulate the water management system. One important requirement of these models is the capability to simulate stream-aquifer interaction or stream-wetland interaction. A significant part of the South Florida landscape is covered with a network of canals that extends for thousands of miles through wetlands, agricultural areas, and urban areas. The behavior of water levels in the canals, when areas adjacent to canals are subjected to water-level changes, is not completely understood. The influences of the highly conductive surface aquifer and the less conductive bottom sediment layer of the canal on the overall hydrology are also not completely known. These behaviors influence a significant part of South Florida hydrology. The current study provides a method to understand the basic parameters that govern the problem and to obtain an analytical solution.

Stream-aquifer and stream-wetland interactions have previously been studied by a number of researchers. The study by Pinder and Sauer (1971) was conducted by using a coupled numerical model for canal flow and 2D groundwater flow. The objective was to study the influence of bank storage on the modification of flood waves. The example used by Pinder and Sauer (1971) served as a benchmark test for integrated models such as MODBRANCH (Swain and Wexler 1996) and MODNET (Walton et al. 1999). These models consist of a MODFLOW model (McDonald and Harbaugh 1988) coupled with either the BRANCH model (Schaffranek 1987) or the UNET model (HEC 1996). The comparison between the solution obtained by Pinder and Sauer (1971) and the solutions obtained using MODBRANCH or MODNET was not perfect because the comparison was between two numerical models, and neither of the solutions has been verified against an analytical solution. The test conditions explained by Pinder and Sauer (1971) are also not completely known. Other researchers who developed integrated models or simply incorporated bank storage effects into stream flow simulations include Zitta and Wiggert (1971) and Morel-Seytoux (1975).

Many research efforts have focused on understanding stream-aquifer interaction at a given canal cross section. Bouwer (1965) analyzed many of the conditions involved with this problem. Dillon and Liggett (1983) used a boundary integral method to determine stream-aquifer interaction in the 2-D domain of the cross section and identify conditions under which the canal and the aquifer are hydraulically disconnected. More recently, Zlotnik and Huang (1999), Moench and Barlow (2000), and others studied stream-aquifer interaction due to step responses in water level fluctuations. A number of streambed sediment layer types and aquifer configurations were used in these studies. They used the 1D equations in the aquifer to study the effect of canal level fluctuations. In the applications by Morel-Seytoux (1975), Swain and Wexler (1996) and others, a simple equation was used to represent sediment resistance. Chin (1990), Genereux and Guardiario (1998) and others extended these basic resistance equations to obtain analytical and semianalytical expressions that can be used with regional models having large cells. Jorgensen et al. (1989) demonstrated the need for care when applying basic seepage equations to models with large cells. Formulations proposed by Chin (1990) and others are partly intended to circumvent some of these problems. The studies carried out in South Florida by Chin (1990), Genereux and Guardiario (1998), Swain and Wexler (1996) and others were triggered by the need to understand the extent of stream-aquifer interaction resulting from the highly permeable limestone-based aquifers. Transmissivities in excess of 1 m^2/s are common in South Florida (Fish and Stewart 1991).

In the current study, coupled equations for canal flow and 2D groundwater flow are analyzed. Resistance of an optimal sediment layer between them is also considered. Approximate analytical solutions are obtained for the equations using Fourier analysis. Two special cases of the solution are used to analyze the behavior of canal and aquifer water levels when the canal upstream boundary water level is varied in a sinusoidal manner, and the behavior of canal and aquifer water levels with time when the initial water surface profile in the

[1]Lead Civ. Engr., South Florida Water Mgmt. Dist., 3301 Gun Club Rd., West Palm Beach, FL 33406.

Note. Discussion open until December 1, 2001. To extend the closing date one month, a written request must be filed with the ASCE Manager of Journals. The manuscript for this paper was submitted for review and possible publication on September 3, 1999; revised February 12, 2001. This paper is part of the ***Journal of Hydraulic Engineering***, Vol. 127, No. 7, July, 2001. ©ASCE, ISSN 0733-9429/01/0007-0567–0576/$8.00 + $.50 per page. Paper No. 21769.

canal is sinusoidal. The analytical solution of problem was then compared with MODFLOW and HSE solutions (Lal 1998b) to show the close agreement of the results.

Results of the study indicate that a number of dimensionless parameter groups can be identified as characterizing the dynamic behavior of stream-aquifer interaction. Values of these parameter groups are obtained for two sites in South Florida that are investigated for stream-aquifer interaction. The influence of the sediment layer which partially insulates the canals, is also described using a parameter group.

Results of the study can be used to develop benchmark test problems with analytical solutions. These problems can be used to verify existing and future models that are used to simulate stream-aquifer interaction. The results of the study can also be combined with results of error analysis (Lal 2000) to determine space and time discretizations needed for numerical models simulating stream-aquifer interaction.

GOVERNING EQUATIONS

Equations describing 2D groundwater flow, 1D canal flow, and resistance to flow across the bottom sediment layer are considered to be the principal relationships that govern the problem of stream-aquifer interaction. The equation describing unsteady flow in a 2D isotropic aquifer is

$$s_c \frac{\partial H}{\partial t} = \frac{\partial}{\partial x}\left(T_g \frac{\partial H}{\partial x}\right) + \frac{\partial}{\partial y}\left(T_g \frac{\partial H}{\partial y}\right) \tag{1}$$

subjected to suitable initial and boundary conditions. In the equation x, y = distances along horizontal x- and y-axes; t = time; H = water head; T_g = transmissivity of the aquifer; and s_c = storage coefficient. For unconfined flow, $T_g \approx k_g h$ where k_g = hydraulic conductivity and h = aquifer thickness.

After neglecting the inertia terms, the Saint Venant equations for a 1D wide rectangular canal are given by

$$\frac{\partial h}{\partial t} + \frac{\partial q}{\partial x} - q_l = 0 \tag{2}$$

$$\frac{\partial h}{\partial x} + S_f - S_0 = 0 \tag{3}$$

where h = water level in the canal; q = discharge rate in the canal per unit width; q_l = total seepage into the canal per unit length per unit width of the canal; and S_0 = bottom slope. The friction slope S_f can be explained using the following general expression:

$$S_f = C \frac{u^n}{h^m} = C \frac{q^n}{h^{m+n}} \tag{4}$$

where u = flow velocity; C = a roughness constant; and m, n = constants. Eq. (4) can be used to represent the Manning's equation using $n = 2$, $m = 4/3$. For Chezy's equation, $n = 2$, $m = 1$.

Seepage between the canal and the aquifer at the aquifer-sediment interface is based on Darcy's law and the Dupuit assumption. The seepage per unit width of the aquifer per unit width of the canal q_l is (Fig. 1)

$$q_l = \frac{2T_g}{B}\left(\frac{\partial H}{\partial y}\right)_{y=\delta+} \tag{5}$$

where B = width of the canal; δ = thickness of the sediment layer when a sediment layer is present; and $(\partial H/\partial y)$ = head gradient near the aquifer at the aquifer-sediment interface. When there is no sediment layer, $\delta = 0$ and the gradient is computed in the aquifer at the aquifer-canal interface.

When a sediment layer is present, the resistance to flow across the layer has to be taken into account. If the sediment layer conductivity is k_m, an equation can be written for seepage assuming that water is not stored in the thin sediment layer (Pinder and Sauer 1971)

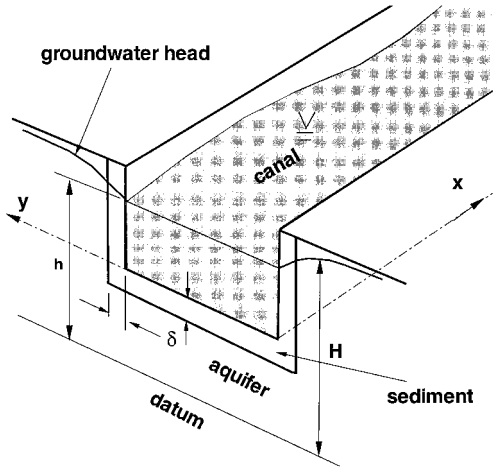

FIG. 1. Aquifer and Canal with Sediment Layer

$$q_l = \frac{2T_m}{B}\left(\frac{\partial H}{\partial y}\right)_{y=\delta-} \approx k_m \frac{p}{B}\frac{\Delta H}{\delta} \tag{6}$$

where $(\partial H/\partial y)_{y=\delta-}$ represents the head gradient in the sediment; T_m = a parameter describing sediment resistance; p = length of wetted perimeter of the canal along which there is seepage; and ΔH = head difference across the sediment layer. For a rectangular canal with seepage from both bottom and sides $p = B + 2d$ in which d = depth. The parameter T_m makes it possible to encapsulate k_m, p, B, canal penetration into aquifer, and any other sediment information into one variable that has units of transmissivity. The parameter T_m is used to represent the resistance to seepage through the bottom, sides, or both, even when the sediment layer thickness and the pressure around it is not uniform. In computing T_m using the approximate relationship shown, it was assumed that the layer thickness and the head gradient are constant, and that the gradient can be approximated using $\Delta H/\delta$. As a result of the assumptions used in computing T_m, its value can be uncertain. However, Pinder and Sauer (1971), Swain and Wexler (1996), Genereux and Guardiario (1998), Chin (1991) and others used similar approaches to characterize the resistance of the sediment layer. Values of k_m/δ described in the equation are available for some areas of South Florida. If the seepage occurs from the canal bottom alone ($p = B$), T_m is obtained using

$$T_m \approx 0.5 p k_m \tag{7}$$

If the canal fully penetrates the aquifer, $p \approx 2d$. Other configurations of the stream-aquifer interface are described in papers including one by Zlotnik and Huang (1999).

METHOD OF SOLUTION

A solution is obtained for the governing equations (1), (2), and (3) assuming that the canal has a uniform cross section and a uniform slope, the canal extends to infinity in the downstream direction, and the aquifer is semiinfinite in the same direction. Perturbation equations are generated for the governing equations by setting the variables to steady state values $H = H_0$, $h = h_0$, and $q = q_0$ as well as slightly perturbed values $H = H_0 + H^*$, $h = h_0 + h^*$ and $q = q_0 + q^*$. The perturbation equations for (1), (2), and (3) are, respectively

$$\frac{\partial}{\partial x}\left(T_g \frac{\partial H^*}{\partial x}\right) + \frac{\partial}{\partial y}\left(T_g \frac{\partial H^*}{\partial y}\right) = s_c \frac{\partial H^*}{\partial t} \tag{8}$$

J. Hydraul. Eng., 2001, 127(7): 567-576

$$\frac{\partial h^*}{\partial t} + \frac{\partial q^*}{\partial x} - \frac{2T_g}{B}\left(\frac{\partial H^*}{\partial y}\right)_{y=\delta+} = 0 \quad (9)$$

$$\frac{\partial h^*}{\partial x} + S_f\left[n\frac{q^*}{q_0} - (m+n)\frac{h^*}{h_0}\right] = 0 \quad (10)$$

Ponce et al. (1978) and Samuels and Skells (1990) have also obtained perturbation equations for canal flow.

Solutions of the exponential form are assumed for the perturbation equations. These solutions guarantee that there are no discontinuities at the canal-sediment and sediment-aquifer interfaces. The solutions are as follows:

$$\text{canal:} \quad h^*(x, t) = h' \exp(ft + \lambda x) \quad (11)$$

$$\text{sediment:} \quad H^*(x, y, t) = h' \exp(ft + \lambda x + \theta y) \quad \text{for} \quad 0 < y \le \delta \quad (12)$$

$$\text{aquifer:} \quad H^*(x, y, t) = h' \exp[ft + \lambda x + \theta\delta + \mu(y - \delta)] \quad \text{for} \quad y > \delta \quad (13)$$

$$\text{canal flow:} \quad q^*(x, t) = q' \exp(ft + \lambda x) \quad (14)$$

here, f, λ, μ, and θ are complex constants; $f = f_1 + f_2 I$, $\lambda = \lambda_1 + \lambda_2 I$, $\mu = \mu_1 + \mu_2 I$, $\theta = \theta_1 + \theta_2 I$, $I = \sqrt{-1}$ in which the subscripted variables are real. For many problems, λ_1 and μ_1 are the decay constants for water-level disturbances along the canal and the aquifer, λ_2 and μ_2 are the wave numbers of the disturbances along the canal and the aquifer, f_1 is a time decay constant for water level disturbances, and f_2 is a characteristic frequency of the problem. After substituting the solutions (11), (12), (13), and (14), (8), (9), and (10), respectively, become

$$T_g(\lambda^2 + \mu^2) = s_c f \quad (15)$$

$$fh' - \frac{2T_g}{B}\mu e^{\delta\theta} h' + \lambda q' = 0 \quad (16)$$

$$\lambda h' - (m+n)\frac{S_f}{h_0} h' + \frac{S_f n q'}{q_0} = 0 \quad (17)$$

Equating (12) and (13) in (5) and (6)

$$T_g\mu = T_m\theta \quad (18)$$

which gives $\theta = T_g\mu/T_m$ to be used to replace θ in (16). For the homogeneous system of equations (16) and (17) to have a nontrivial solution in $[h', q']$, the determinant of the coefficient matrix must vanish. This condition is given by

$$\left[f - \frac{2T_g}{B}\mu \exp\left(\frac{T_g}{T_m}\mu\delta\right)\right]\frac{S_f n}{q_0} = \lambda\left[\lambda - (m+n)\frac{S_f}{h_0}\right] \quad (19)$$

Eqs. (15) and (19) are the two final equations that describe the propagation of small amplitude waves. Eq. (15) represents the groundwater response and (19) represents the surface water response along the canal. A number of simplifying assumptions can be used to obtain practical solutions to these equations.

Selection of Dimensionless Parameters

Dimensionless variables are used to simplify the governing equations described by (15) and (19). The dimensionless variables are selected so that the final form of the governing equation does not retain too many empirical constants coming from the friction equations. A characteristic length Λ related to the wave number of the water-level disturbance is defined first. It is used to make the other lengths dimensionless. It is defined as

$$\lambda = \sqrt{\frac{q_0}{nS_f f_r}} = \sqrt{\frac{T_c}{nf_r}} \quad (20)$$

in which f_r = a characteristic frequency of the system. The parameter T_c is used to linearize the resistance to flow along the canal. It is similar to aquifer transmissivity and is defined as

$$T_c = \frac{q_0}{S_f} \quad (21)$$

with q_0 being computed using (4). Variables λ and μ are made dimensionless by using $\hat{\lambda} = \lambda\Lambda$, $\hat{\mu} = \mu\Lambda$, and $\hat{x} = x/\Lambda$. Similarly, t and f are made dimensionless using $\hat{t} = f_r t$ and $\hat{f} = f/f_r$. If the system is disturbed by a water-level fluctuation of frequency f_r at the upstream end of the canal, f_2 is considered to be this disturbing frequency ($f_2 = f_r$).

The transmissivity ratio parameter P_r characterizing the transmissivity, storage coefficient, and canal friction is defined using (15) and (20) as

$$P_r = \frac{T_g}{s_c f_r \Lambda^2} = \frac{nT_g S_f}{s_c q_0} = \frac{nT_g}{s_c T_c} \quad (22)$$

The canal-width parameter P_b characterizing the canal width is defined as

$$P_b = \frac{B}{\Lambda s_c} \quad (23)$$

The canal depth parameter P_d characterizing the canal depth and the canal slope is defined as

$$P_d = \frac{h_0}{(m+n)S_f\Lambda} \quad (24)$$

The sediment resistance parameter P_m characterizing the resistance of the sediment layer is defined as

$$P_m = \frac{T_m}{\delta f_r \Lambda s_c} = \left(\frac{k_m}{\delta}\right)\left(\frac{1}{f_r}\right)\left(\frac{B}{\Lambda}\right)\left(\frac{1}{s_c}\right) \quad (25)$$

Variables used to define P_m show that k_m/δ is a parameter that can be used to explain sediment resistance. Using these dimensionless parameters, the system of governing equations (15) and (19) can be reduced to the following form:

$$P_r(\hat{\lambda}^2 + \hat{\mu}^2) = \hat{f} \quad (26)$$

$$\hat{\lambda}^2 - \frac{\hat{\lambda}}{P_d} + \frac{2\hat{\mu}P_r}{P_b}\exp\left(\frac{P_r\hat{\mu}}{P_m}\right) = \hat{f} \quad (27)$$

Eqs. (26) and (27) describe the behavior of small water-level disturbances in the canal under transient conditions. Real and complex components of $\hat{\lambda}$ and $\hat{\mu}$ describe the exponential decay and the wave number, respectively. Variables $\hat{\lambda}$ and $\hat{\mu}$ correspond to the canal and the aquifer, respectively. Real and imaginary components of $\hat{f}$ describe the exponential time decay and the frequency, respectively. The solution depends on P_r, P_b, P_d, and P_m.

SOLUTIONS OF GOVERNING EQUATIONS

Analytical solutions to the governing equations can be obtained only for a number of simple practical problems. These solutions can be obtained by solving (26) and (27) simultaneously for two of the three complex variables $\hat{\lambda}$, $\hat{\mu}$, and $\hat{f}$ when the third is known. The following two problems cover two of these three problem types. A third problem type, involving the determination of $\hat{\lambda}$ and $\hat{f}$ for a known $\hat{\mu}$, is not described in this paper.

J. Hydraul. Eng., 2001, 127(7): 567-576

Problem 1: Behavior of Canal and Aquifer Water Levels When a Small Continuous Sinusoidal Water-Level Disturbance Is Introduced at Upstream Canal Boundary

When a continuous sinusoidal water-level disturbance is introduced at the upstream end of a sloping canal, the wave number λ_2 and the amplitude decay constant λ_1 of the disturbance in the canal can be obtained by solving (26) and (27) simultaneously for a known $f = f_r I$, ($f_1 = 0$, $f_2 = f_r$) in which f_r is the frequency of the disturbance. Since it is not possible to obtain a simple explicit solution, three alternative approaches were used to solve the coupled equations. The first approach was to simply use Mathematica (Wolfram 1996) directly. This method worked, but the symbolic solution was inaccurate for certain ranges of parameters. The second and third solution methods are described next.

Solution 1: Iterative Solution

The iterative method is the most accurate method for a variety of practical problems. It takes advantage of the fact that $\hat{\lambda} << \hat{\mu}$ for groundwater flow. Under such conditions, the system of equations consisting of (26) and (27) can be solved iteratively. The first equation in the iteration is obtained using (26) as

$$\hat{\mu} = -\sqrt{\frac{I}{P_r} - \hat{\lambda}^2} \tag{28}$$

in which $\hat{f} = I$, since $f = f_r I$. The negative roots are selected for both $\hat{\lambda}$ and $\hat{\mu}$ to represent solutions that decay with time and distance. The second equation for the iteration is obtained using (27)

$$\hat{\lambda} = \frac{1}{2P_d} - \sqrt{I + \frac{1}{4P_d^2} - 2\,\frac{\hat{\mu}P_r}{P_b}\exp\left(\frac{P_r\hat{\mu}}{P_m}\right)} \tag{29}$$

Eq. (28) is solved for $\hat{\mu}$ first using $\hat{\lambda}$ from the previous iteration or zero. Eq. (29) is solved next to obtain $\hat{\lambda}$. The value of $\hat{\mu}$ is updated next using (28). The two steps are repeated until the solution converges. In the test problems described later, the analytical solution is obtained using this method.

Solution 2: Approximate Explicit Solution

An approximate explicit solution can be obtained for the coupled equations (28) and (29) by taking advantage of the condition $\hat{\lambda} << \hat{\mu}$ for groundwater flow. This is true when $P_r << 1$. The value of $\hat{\mu}$ is first computed explicitly using (28) after neglecting the value of $\hat{\lambda}^2$. This value of $\hat{\mu}$ is substituted in (29) to obtain the following approximate equation:

$$\hat{\lambda} = \frac{1}{2P_d} - \sqrt{I + \frac{1}{4P_d^2} + 2\,\frac{\sqrt{P_r I}}{P_b}\exp\left(-\frac{\sqrt{0.5P_r}}{P_m}\right)} \tag{30}$$

In the part of the expression $\exp(\hat{\mu}P_r/P_m)$ in (29) which was originally $\exp(\delta\theta)$ in (16), it was assumed that the sediment layer is thin, the storage does not change, and that there is no phase lag when a disturbance passes through it. This assumption is useful in simplifying the solution by neglecting the imaginary part of θ. As a result, it also becomes possible to define a single parameter χ to characterize stream-aquifer interaction. Eq. (30) can now be expressed using χ and P_d only, in which P_d is used to describe the canal hydraulics. The parameter χ is defined as

$$\chi = \frac{P_b}{\sqrt{P_r}}\exp\left(-\frac{\sqrt{0.5P_r}}{P_m}\right) \quad \text{with a sediment layer} \tag{31}$$

$$\chi = \frac{P_b}{\sqrt{P_r}} \quad \text{without a sediment layer} \tag{32}$$

The parameter χ consists of two groups of variables. The group $P_b/\sqrt{P_r}$ describes the canal and aquifer characteristics. The group $\exp(-\sqrt{0.5P_r/P_m})$ describes the characteristics of the sediment layer. The influence of the sediment layer is simply to modify χ by the term $\exp(-\sqrt{0.5P_r/P_m})$. When this latter term is zero, $\chi = 0$, and the canal is completely isolated or cutoff from the aquifer. The influence of the sediment layer on insulating the canal from the aquifer is described later.

Behavior of the Solution

Analytical solutions with real and imaginary components of $\hat{\lambda}$ and $\hat{\mu}$ are plotted in Figs. 2 and 3, respectively. They are obtained using (30). Both graphs show that small values of χ give large negative values of $\hat{\lambda}$ implying large decays in water-level disturbances. Both graphs show that in relatively deep flat canals ($P_d > 0.5$), the dependence of the solution on χ ceases when χ is greater than about 10. This shows that water-level disturbance characteristics in the canal are unaffected by its interaction with the aquifer for large values of χ and P_d. This zone of no interaction is the zone in which $\hat{\lambda}$ lines are parallel to the χ axis. Eq. (30) also shows that when

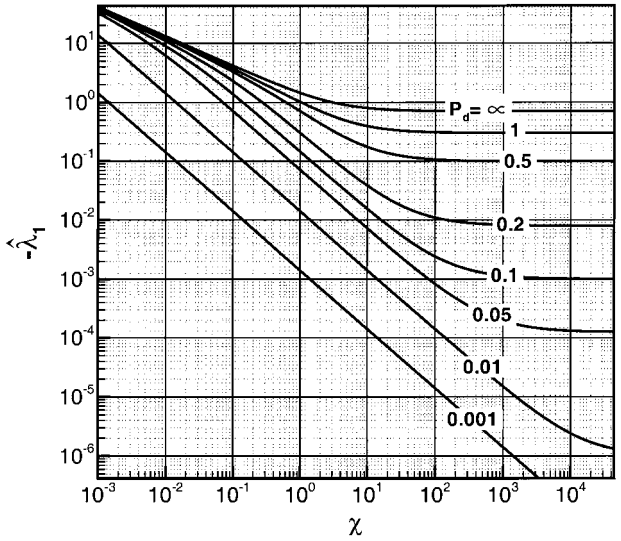

FIG. 2. Variation of $-\hat{\lambda}_1$ with χ Obtained Using Analytical Solution

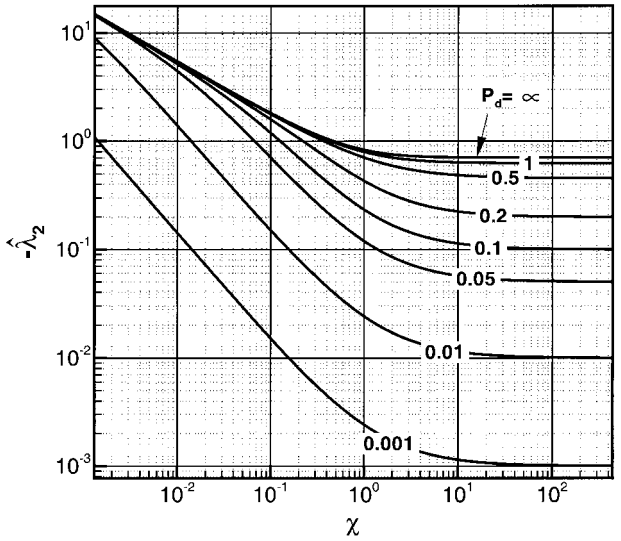

FIG. 3. Variation of $-\hat{\lambda}_2$ with χ Obtained Using Analytical Solution

J. Hydraul. Eng., 2001, 127(7): 567-576

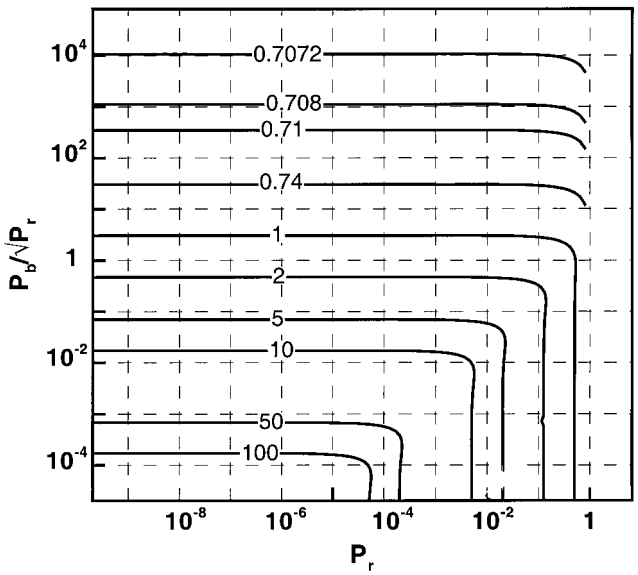

FIG. 4. Variation of $-\hat{\lambda}_1$ with P_r and $P_b/\sqrt{P_r}$

$P_b/\sqrt{P_r} \to \infty$, the solution $\hat{\lambda}$ is a function of P_d only. If the canal is very deep and the bottom slope is small, $P_d \to \infty$, and $\hat{\lambda} = -(1 + I)/\sqrt{2}$ as seen in both plots.

When P_d and P_b are very large and λ^2 is very small, $\hat{\mu}$ in (28) can be used in (30) to obtain an order of magnitude estimate for $\hat{\mu}/\hat{\lambda}$ as $1/\sqrt{P_r}$. This is the ratio between wave lengths in the canal and the aquifer when $P_r << 1$ and $\hat{\mu} >> \hat{\lambda}$.

Instead of using the approximate solution of (30), if the complete equations (26) and (27) are solved using the iterative method, the plot in Fig. 4 can be obtained. In this figure, $-\hat{\lambda}_1$ is plotted against P_r and $P_b/\sqrt{P_r}$. This figure is useful in understanding the range of validity of the approximate solution of (30) shown in Figs. 2 and 3. Fig. 4 shows that $\hat{\lambda}_1$ is a function of χ and $P_b/\sqrt{P_r}$ over only a large but limited range indicated by the area in which all the curves are parallel to the P_r axis. If P_r is too large (>0.1 for most practical purposes), $-\hat{\lambda}_1$ is not a function of $P_b/\sqrt{P_r}$ alone, and (30) becomes inaccurate. Large values of P_r imply a violation of the assumption $\lambda << \mu$ (or $T_g << T_c$) that was used to obtain the approximate form (30).

Insulating Effect of the Sediment Layer

In the governing equations, sediment-layer characteristics are described using the dimensionless parameter group $\sqrt{0.5P_r}/P_m$. When the sediment layer conductivity is large or the sediment layer is thin, $\sqrt{0.5P_r}/P_m$ becomes small and the $\exp(-\sqrt{0.5P_r}/P_m)$ term in (30) or the $\exp(\delta\theta)$ term in (16) comes closer to 1. When this happens, χ becomes equal to $P_b/\sqrt{P_r}$, and the sediment layer ceases to have any influence on the solution of $\hat{\lambda}$.

When the sediment-layer conductivity becomes small or the sediment layer thickness becomes large, the term $\exp(-\sqrt{0.5P_r}/P_m)$ in (30) or $\exp(\delta\theta)$ in (16) becomes small. Only a portion of the hydrostatic pressure disturbance in the canal will be transmitted to the aquifer at this point. At the limit of $\chi \to 0$, the canal is fully insulated from the aquifer by the sediment layer and $\hat{\lambda}$ in (30) becomes a function of P_d only.

Eq. (30) shows that many different combinations of $P_b/\sqrt{P_r}$ and $\sqrt{0.5P_r}/P_m$ can give the same χ and therefore the same solution $\hat{\lambda}$. In order to obtain a limiting value for $\sqrt{0.5P_r}/P_m$ at which the sediment layer can just prevent water-level disturbances in the canal from affecting the head disturbances in the aquifer, an arbitrary reduction of χ to 5% is considered. When this happens, $\exp(-\sqrt{0.5P_r}/P_m) = 0.05$ or $\sqrt{0.5P_r}/P_m = 3$. This condition can be used to define an approximate hydraulic cutoff point between the canal and the aquifer. This condition is

$$\frac{P_m}{\sqrt{0.5P_r}} < \frac{1}{3} \tag{33}$$

When this condition is met, water-level disturbances in the canal are relatively unaffected by the aquifer. The disturbances are not felt outside the sediment layer, and aquifer properties do not affect the solution. The canal then acts as if it runs through an aquifer made of the sediment material. Eqs. (28) and (29) are valid for the entire canal-aquifer-sediment system only when there is no hydraulic cutoff.

Physical Characteristics of Small Water-Level Disturbances

The solutions $\hat{\lambda}$ and $\hat{\mu}$ can be used to determine many physical characteristics of small-amplitude water-level disturbances. Table 1 shows some of the expressions that were used to determine these characteristics. The logarithmic decrement mentioned in the table is measured using the amplitudes of two consecutive cycles and can be used to quantify decay. Some of the definitions used in the table were obtained using Wylie (1979) and Ponce et al. (1978). The physical characteristics listed in the table can be measured in the field or computed using numerical models. The accuracy of numerical models can be estimated by comparing the analytical and model values of these properties.

Problem 2: Behavior of a Sinusoidal Small-Amplitude Water Surface Profile in a Canal with Time

The governing equations (26) and (27) can be solved for $\hat{\mu}$ and $\hat{f}$ if $\hat{\lambda}$ is known. As the first step, $\hat{f}$ is eliminated from (26) and (27) to obtain

$$\hat{\lambda}^2 - \frac{\hat{\lambda}}{P_d} + \frac{2\hat{\mu}P_r}{P_b}\exp\left(\frac{P_r\hat{\mu}}{P_m}\right) = P_r(\hat{\lambda}^2 + \hat{\mu}^2) \tag{34}$$

This equation is solved for $\hat{\mu}$ assuming $\hat{\lambda}$ is in the form $\hat{\lambda}_2 I$ where $\hat{\lambda}_2$ is a dimensionless wave number. An explicit solution can be obtained when there is no sediment layer by solving the quadratic equation to obtain

$$\hat{\mu} = \frac{1}{P_b} - \sqrt{\frac{1}{P_b} - \frac{\hat{\lambda}}{P_r P_d} + \frac{\hat{\lambda}^2}{P_r}} \tag{35}$$

The parameter $\hat{f}$ can then be determined by using (26).

TEST PROBLEMS

Two numerical models were used with two test problems to determine how the analytical solutions derived earlier under Problem 1 would compare with the numerical solutions. The

TABLE 1. Mathematical Expressions Used to Describe Physical Characteristics of Small Amplitude Water Level Disturbances Traveling down a Canal

Description	Expression
Variation of the amplitude of water level in the canal	$H_0 \exp(-\hat{\lambda}_1\hat{x})$
Variation of the amplitude of water head in the aquifer perpendicular to the canal	$H_0 \exp(-\hat{\mu}_1\hat{y})$
Speed of disturbance along the canal (dimensionless)	$1/\hat{\lambda}_2$
Speed of disturbance along the canal (dimensional)	$f_r\Lambda/\hat{\lambda}_2$
Speed of disturbance in the aquifer perpendicular to the canal (dimensionless)	$1/\hat{\mu}_2$
Speed of disturbance in the aquifer perpendicular to the canal (dimensional)	$f_r\Lambda/\hat{\lambda}_2$
Logarithmic decrement (Wylie 1979)	$2\pi\lambda_1/\lambda_2$

J. Hydraul. Eng., 2001, 127(7): 567-576

numerical models used were the MODFLOW model (McDonald and Harbaugh 1988), and the Hydrologic Simulation Engine (HSE) (Lal 1998b; Lal et al. 1998c). HSE is an implicit finite-volume model with fully coupled 2D overland flow, groundwater flow, and canal flow features. One of the test problems used was similar to the problem used by Pinder and Sauer (1971). The discretizations used were somewhat crude to allow for timely completion of the experiments.

Tests Using MODFLOW Model

A single-layer 2D MODFLOW model was used to solve the first test problem and determine the exponential decay constant $\hat{\lambda}_1$ in the canal. Fig. 5 shows the cell configuration used, with cells fully covering the canal and the 50 km $\times$ 50 km, square-shaped, confined aquifer. The aquifer was discretized using 1,000 m $\times$ 1,000 m cells. The canal and the sediment layers were represented using four rows of cells. Different canal and sediment layer widths needed for the experiment were obtained by using different cell widths. No-flow boundaries were assumed at the outside boundaries. Instead of a nonlinear, Manning-type friction equation, a linear friction equation such as (4) was used with $n = 1$ and $m = 0$. Eq. (21) was used to compute the constant T_c.

During the experiments, the water level at the upstream boundary of a horizontal canal was varied continuously in a sinusoidal manner. Different periods of oscillation were used for different test runs. The upstream amplitude was maintained as 1.0 m, which is small compared to the aquifer depth of 50.0 m. To establish the initial condition, sinusoidal water-level variations were maintained at the upstream end for some time until the wave shapes at a downstream point become consistently similar. The time step used was 1/50th of the period of oscillation. The exponential decay rate of the sinusoidal wave in the canal was obtained by measuring the amplitude of water-level variation along the canal at a number of points and plotting its log value against distance. Approximately 10–50 cycles of sine waves were allowed to pass before a stable data set could be obtained. The parameters needed for the experiment were selected so that the solution does not extend too close to the boundary.

Test with Varying P_b

This test was conducted to determine whether the analytical solution developed earlier can accurately predict the solution describing the decay rate $\hat{\lambda}_1$ and the wave number $\hat{\lambda}_2$ obtained by using MODFLOW model runs. The results were plotted against various canal widths or P_b to see the agreement. In the test P_r was maintained at two constant values 1.0×10^{-2} and 1.0×10^{-3}, and for each value model runs were made using different P_b. A sediment layer was not used. The parameters for this experiment are shown in Table 2. High values of transmissivities exceeding 1 m^2/s are common in South Florida as described by Fish and Stewart (1991), Chin (1991), and Genereux and Guardiario (1998). The reason for the severity of the stream-aquifer interaction also has to do with the high transmissivity of the aquifer. Large values of transmissivities chosen for the experiment helped to increase the range of dimensionless parameters used in the experiment as well. Fig. 6 shows the agreement of analytical and numerical results. These results show a reduction of the decay when the width is increased. The analytical solutions were obtained using the iterative method.

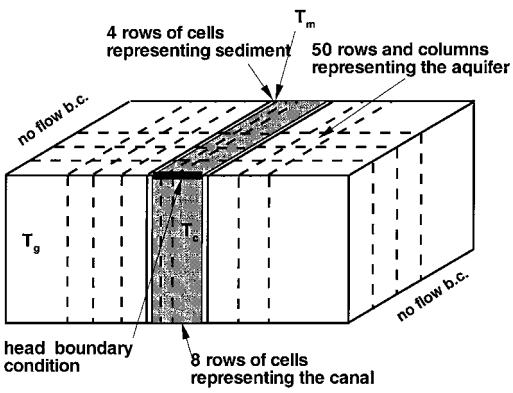

FIG. 5. MODFLOW Grid Used in the Test Problem

TABLE 2. Data Values Used for Test Problem 1, Cases 1 and 2 with MODFLOW Model [T = Wave Period (s); T_g = Aquifer Transmissivity (m^2/s); T_c = Equivalent Transmissivity of Canal as Defined in Eq. (21) (m^2/s); s_c = Storage Coefficient; and B = Canal Width (m)]

T	T_g	T_c	s_c	B	Λ (m)	P_r	P_b	$\hat{\lambda}$
(a) Case 1								
10^8	10^{-3}	1	0.1	400.0	3,997	10^{-2}	1.00	0.79
10^8	10^{-3}	1	0.1	160.0	3,997	10^{-2}	0.40	0.86
10^8	10^{-3}	1	0.2	40.0	3,997	10^{-2}	0.05	1.75
10^8	10^{-3}	1	0.1	8.0	3,997	10^{-2}	0.02	2.65
10^8	10^{-3}	1	0.1	40.0	3,997	10^{-2}	0.10	1.31
10^8	10^{-3}	1	0.1	80.0	3,997	10^{-2}	0.2	1.03
10^6	0.2	1,000	0.1	40.0	12,616	10^{-3}	0.032	1.31
10^6	0.2	1,000	0.5	400.0	12,616	10^{-3}	0.063	1.036
10^6	0.2	1,000	0.2	400.0	12,616	10^{-3}	0.159	0.842
10^6	0.2	1,000	0.2	40.0	12,616	10^{-3}	0.0159	1.757
(b) Case 2								
10^6	0.2	1,000	0.2	126.1	12,616	10^{-3}	0.05	1.314
10^6	0.02	1,000	0.2	126.1	12,616	10^{-4}	0.05	0.891
10^6	0.002	1,000	0.2	126.1	12,616	10^{-5}	0.05	0.756
10^6	0.0002	1,000	0.2	126.1	12,616	10^{-6}	0.05	0.709
10^6	1.0	1,000	0.2	126.1	12,616	0.005	0.05	1.683

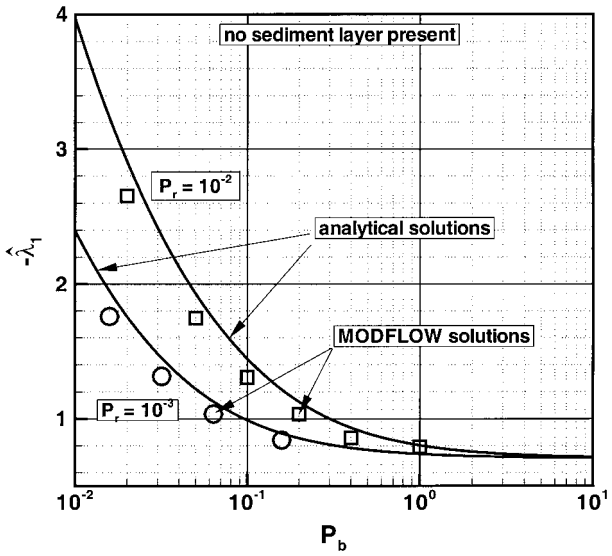

FIG. 6. Comparison of $-\hat{\lambda}_1$ Obtained Using Analytical Method and MODFLOW Model for $P_r = 10^{-2}$ and $P_r = 10^{-3}$ without a Sediment Layer

The differences between the results of the numerical model (MODFLOW, HSE) and the analytical method can be due to a number of reasons. The results are different primarily due to the difficulty of representing an analytical problem exactly using a numerical model. The results are different due to the numerical errors resulting from relatively crude discretization as well. Fine resolutions are sometimes prohibitive due to excessive run times (Lal 1998a, 2000). Numerical errors exist in problems with boundaries at infinity, because models have finite grids that do not extend to infinity. Difficulty of obtaining accurate initial conditions for the numerical models is another

reason for the difference. Methods used to compute $\hat{\lambda}$ from the results of numerical models can also introduce errors.

Test with Varying P_r

This test was carried out to determine if the analytical and numerical solutions agree for a number of conditions under which P_r or the transmissivity ratio is varied while maintaining P_b at 0.05. Fig. 7 shows the variation of $\hat{\lambda}_1$ with P_r. The differences between analytical and numerical solutions can be attributed to numerical and other errors explained earlier in the previous section. Table 2 shows the parameters used in the model runs.

Test with Varying P_m

This test was carried out to determine if the analytical and numerical solutions agree when the bottom sediment resistance P_m is varied while keeping values of P_r and P_b constant at 0.1 and 0.25, respectively. Fig. 8 shows the variation of $\hat{\lambda}_1$ with P_m. Table 3 shows the values of the parameters used. Fig. 8 shows that the decay of a disturbance measured by $\hat{\lambda}_1$ increases as k_m/δ is increased. In Fig. 8 the point at which the canal becomes completely insulated is described by (33) as $P_m \approx 0.22$. The anomaly in the data point corresponding to $P_m = 0.06$ shows that $\hat{\lambda}_1$ is independent of P_m when the canal is fully insulated. It shows that the same analytical solution is discontinuous at the cutoff.

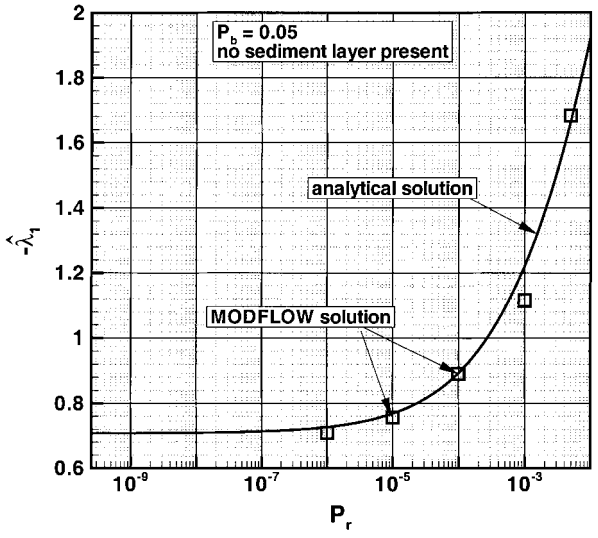

FIG. 7. Comparison of $-\hat{\lambda}_1$ versus P_b Curves Obtained Using Analytical Method and MODFLOW Model for $P_b = 0.05$ and No Sediment Layer

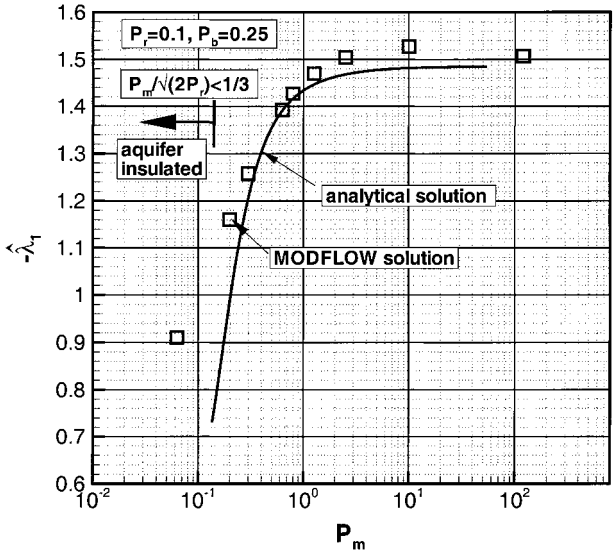

FIG. 8. Comparison of $-\hat{\lambda}_1$ versus P_m Curves Obtained Using Analytical Method and MODFLOW Model for $P_r = 0.1$, $P_b = 0.25$, and No Sediment Layer

TABLE 3. Data Values Used for Test Problem 1, Case 3 with MODFLOW Model T_m = Equivalent Transmissivity of Sediment (m^2/s) and $P_r = 0.1$, $P_b = 0.25$, $s_c = 0.2$, and $\Lambda = 12{,}616$ m for All Cases; in MODFLOW Model, $T_g = 20$ m^2/s, $\delta = 20.0$ m, $T_c = 1{,}000$ m^2/s, $B = 630.4$ m, and $T = 10^6$ s]

T_m	P_m	λ_1
20	126.0	1.506
0.2	0.631	1.393
0.02	0.063	0.910
0.4	1.262	1.469
0.8	2.523	1.504
3.17×10^{-4}	1.0×10^{-3}	0.7513
0.254	0.8	1.427
0.0951	0.3	1.258

Tests Using HSE Model

These tests are very similar to the ones performed by Pinder and Sauer (1971) with their model, by Swain and Wexler (1996) with the BRANCH model (Schaffranek 1987) and by Walton et al. (1999) with the UNET (HEC 1996) model. The objective is to determine whether the analytical and numerical solutions agree under a variety of test conditions. These tests are useful in verifying the accuracy of numerical models. The original problem by Pinder and Sauer (1971) had a number of unknown conditions and did not have an analytical solution. Following is a modified version of the original problem that is easier to set up.

As in the original problem, the modified system has a flood plain that is 39,624 m (130,000 ft) long, 427 m (1,400 ft) across the valley, and surrounded by an impermeable boundary on all sides. The hydraulic conductivity of the aquifer is 3.048×10^{-3} m/s (0.01 ft/s), and the aquifer storage coefficient is 0.25. The aquifer is confined, 67.05 m (220 ft) thick at the upstream boundary, and 27.43 m (90 ft) deep at the downstream boundary. The channel is located at the center of the aquifer parallel to its longer side. It has a slope of $S_0 = 0.001$, width of $B = 30.48$ m (100 ft), and a Manning roughness of 0.03858. The uniform flow depth is $h_0 = 6.09$ m (20 ft) computed for a discharge rate of 509.7 m^3/s (18,000 ft^3/s) in the canal. The hydraulic depth is assumed to equal the actual canal depth to make this application compatible with the MODBRANCH application by Swain and Wexler (1996). Seepage is assumed to occur only from the bottom. The downstream boundary is assumed to have uniform flow at a slope of 0.001. The triangular cell discretization for the problem has right-angled triangles 609.6 m long in the direction of the canal and 15.24 m across. The MODBRANCH model explained earlier has rectangular cells with the same dimensions. The time step is 5 min. Two of the tests carried out with the HSE model are described next.

Test to Compare Water Levels Computed Numerically and Analytically

The purpose of this test is to compare the water levels computed using the HSE model with the water levels computed using the analytical method. The flood hydrograph introduced at the upstream boundary condition is

$$Q = 509.70 + 141.58 \sin\left(\frac{2\pi t}{T_p}\right) \tag{36}$$

J. Hydraul. Eng., 2001, 127(7): 567-576

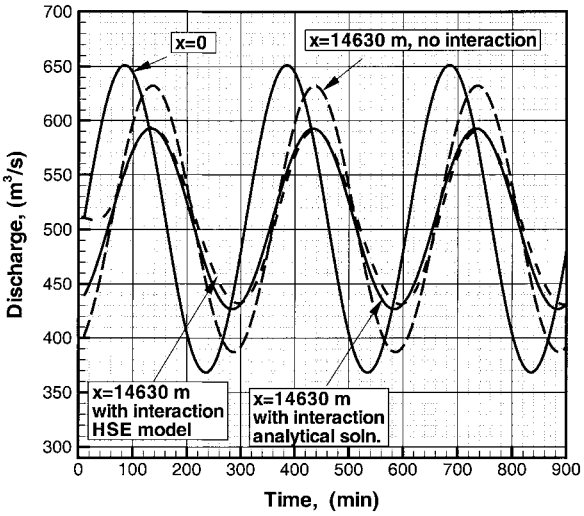

FIG. 9. Variation of Water Level at $x = 0$ m and $x = 14{,}630$ m Obtained Using HSE Model with and without Stream-Aquifer Interaction

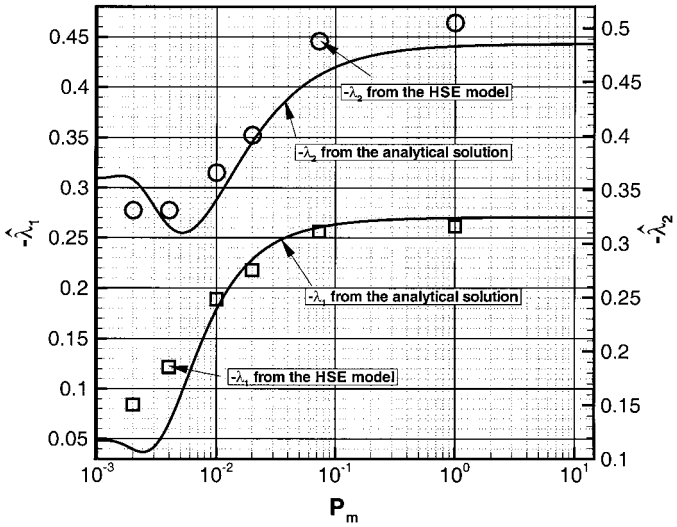

FIG. 10. Comparison of $-\hat{\lambda}_1$ versus P_m and $-\hat{\lambda}_2$ versus P_m Curves Obtained Using Analytical Method and HSE Model ($P_d = 0.3737$, $P_r = 9.78 \times 10^{-5}$, $P_b = 2.49 \times 10^{-2}$)

where T_p = period of the disturbance = 5 h. According to the conditions derived by Ponce et al. (1978), this problem can be solved using a diffusion model such as HSE. Fig. 9 shows output discharge rates in the canal computed at a distance of 14,630 m (48,000 ft) along the canal. The analytical solution is obtained using the following parameters: $f_r = 3.49 \times 10^{-4}$ s^{-1}; $q_0 = Q/B = 509.7/30.48 = 16.72$ m^2/s; $S_f = 0.001$; $n = 2$. When used with these values, (20) gives $\Lambda = 4894.3$ m; (23) gives $P_b = 0.0249$; (24) with $m = 1.333$ gives $P_d = 0.3737$. Considering that the transmissivity $T_g = 0.204$ m^2/s, P_r can be computed as 9.779×10^{-5}. Solving (28) and (29) for $k/\delta = 2.803 \times 10^{-4}$, ($P_m = 0.01$), it is possible to obtain $\hat{\lambda}_1 = -0.1785$, $\hat{\lambda}_2 = -0.3409$, $\hat{\mu}_1$, = $\hat{\mu}_2 = -71.5$. These values are used to obtain the analytical solution for the discharge at a distance x from the upstream boundary as

$$Q = 509.7 + 141.58 \exp\left(\frac{\hat{\lambda}_1 x}{\Lambda}\right) \sin\left(f_r t + \frac{\hat{\lambda}_2 x}{\Lambda}\right) \qquad (37)$$

When there is no interaction with the groundwater aquifer, $\hat{\lambda}_1 = -4.779 \times 10^{-2}$ and $\hat{\lambda}_2 = -0.3608$. These values, when compared with $\hat{\lambda}_1 = -0.1785$ and $\hat{\lambda}_2 = -0.3409$, show that the decay rate of the amplitude in the canal is significantly affected by its interaction with the aquifer. Similarly, the wave period, represented by $\hat{\lambda}_2$, changes from -0.3409 to -0.3608, indicating that there is a slowdown. Analytical solutions of $\hat{\mu}_1 \approx \hat{\mu}_2 \approx -71.5$ can be obtained using (29).

Test with Varying P_m

This test was conducted to determine whether the $\hat{\lambda}_1$ and $\hat{\lambda}_2$ values computed using the HSE model agree with the analytical solutions. During the tests P_m, representing the sediment resistance, was varied while maintaining other parameters constant. The HSE model value of $\hat{\lambda}_1$ was computed by monitoring the output to obtain discharge time series at two arbitrary points along the canal. The ratio of amplitudes at these points can be shown to be $y_2/y_1 = \exp[-\lambda_1(x_2 - x_1)]$ which can be used to compute $\hat{\lambda}_1$. For the current test $x_1 = 609.6$ m and $x_2 = 609.6 \times 25 = 15{,}240$ were used. The value of λ_2 was determined by measuring the time of travel of a peak. Fig. 10 shows that the values of λ_1 and λ_2 obtained analytically and numerically using the HSE model agree approximately. The difference between the values can be due to numerical errors and other problems mentioned earlier.

The analytical solution for $\hat{\mu}_2$ can be used to obtain $\mu_2 = \hat{\mu}_2/\Lambda = 0.01461$. This gives the wave length of the disturbances in the aquifer perpendicular to the canal as 430 m. For a 0.16% error in spatial representation and a <5% computational error margin, Lal (2000) showed that $\Delta y < 0.2/\mu_2 = 0.2/0.0146 = 13.7$ m. Comparing the result with a value of 15.2 m used in the numerical model, the cell size can be considered as adequate. Lal (2000) also showed that the maximum distance of propagation in the aquifer before the amplitude decays to less than 5% of its initial value is $\approx 3/\mu_2 = 205$ m. This value is approximately equal to half the width of the test bed used.

APPLICATIONS

The analytical equations derived in the paper are applied to evaluate stream-aquifer interaction at two sites in South Florida. The L31N canal and the Snapper Creek Extension (SNE) canal are chosen for the purpose. These two canals have been studied extensively for seepage related issues (Chin 1991). Based on this reference, parameter values assumed for the L31N canal are: $q_0 = 0.388$ m^3/s; $B = 27$ m; $h_0 = 4.16$ m; Manning's constant = 0.025; $S_f = 8.14 \times 10^{-7}$; $k_m/\delta = 1.36 \times 10^{-3}$ s^{-1}; $T_g = 1.29$ m^2/s; and $s_c = 0.2$. Parameter values assumed for the SNE canal are: $q_0 = 0.415$ m^3/s; $B = 15$ m, $h_0 = 6.03$ m; Manning's constant = 0.025; $S_f = 2.72 \times 10^{-7}$; $k_m/\delta = 1.49 \times 10^{-3}$ s^{-1}; $T_g = 1.075$ m^2/s; and $s_c = 0.2$.

Table 4 shows some of the derived parameters when the periods of water level disturbance are 1 day, 7 days, and 30 days. In the table, subscript (no-int) refers to cases where the stream-aquifer interaction is suppressed. Then, variables ΔL and Δy are spatial discretizations to represent the sinusoidal solution in the canal and the aquifer, respectively. They are calculated using the methods suggested by Lal (2000). The spatial discretization used for the canal and the aquifer are $0.2/\lambda_2$ and $0.2/\mu_2$, respectively, for the representational errors not to exceed 0.16% and the computational errors not to exceed 5%. The time step was $0.2/f_2$, in which f_2 is the frequency of the disturbance. The parameters $L_{0.5}$ and $y_{0.5}$ give the distances at which the wave amplitude in the canal and the aquifer has decayed to 50% of its original value. The sediment layer is responsible for reducing the amplitude by a factor $\exp(\delta\theta)$ or $\exp(-\sqrt{0.5P_r/P_m})$.

The table shows that there is a significant decay of water-level fluctuations along the canal due to its interaction with the aquifers. A disturbance that has a period of 1 day would travel 57.7 km before a 50% decay in amplitude in a lined L31N canal, and the same would travel only 20.7 km in an

J. Hydraul. Eng., 2001, 127(7): 567-576

TABLE 4. Table of Parameter Values Used for L31N and Snapper Creek Extension (SNE) Canals in South Florida

Variable	L31N			Snapper Creek		
T_p (days)	1	7	30	1	7	30
Λ (m)	57,280	151,550	313,750	102,550	271,260	561,670
P_r	2.703×10^{-5}	2.703×10^{-5}	2.703×10^{-5}	7.031×10^{-6}	7.031×10^{-6}	7.031×10^{-6}
P_b	2.339×10^{-3}	8.842×10^{-4}	4.274×10^{-4}	7.281×10^{-4}	2.752×10^{-4}	1.329×10^{-4}
P_m	2.181×10^{-2}	5.771×10^{-2}	1.914×10^{-1}	7.449×10^{-3}	1.971×10^{-2}	4.080×10^{-2}
P_d	26.8	10.1	4.9	64.9	24.6	11.9
$\exp(-\sqrt{0.5P_r}/P_m)$	0.845	0.938	0.969	0.777	0.909	0.955
$\hat{\lambda}_1$	1.915	3.113	4.452	2.349	3.960	5.743
$\hat{\lambda}_2$	0.821	1.311	1.884	0.823	1.527	2.306
$\mu_{\hat{\lambda}_1}$	136	136	136	267	267	267
$\mu_{\hat{\lambda}_2}$	136	136	136	267	267	267
$(\hat{\lambda}_1)_{\text{no-int}}$	0.688	0.658	0.608	0.699	0.686	0.665
$(\hat{\lambda}_2)_{\text{no-int}}$	0.707	0.706	0.703	0.707	0.706	0.706
wave length (m)	438,380	726,350	1,046,400	782,750	1,116,180	1,530,110
$L_{0.5}$ (m)	20,700	33,700	48,800	30,254	47,480	67,800
$(L_{0.5})_{\text{no-int}}$ (m)	57,700	160,600	357,800	101,700	274,000	585,000
ΔL (m)	14,000	23,100	33,300	24,921	33,500	48,700
$y_{0.5}$ (m)	292	772	1,599	266	704	1,458
Δy (m)	84	223	461	77	203	421
Δt (days)	0.2	1.4	6.0	0.2	1.4	6.0

unlined L31N canal. The resulting disturbance in the aquifer does not travel very far, as shown by the value of $y_{0.5}$ = 292 m. The discretization in the aquifer in a direction normal to the canal is relatively fine as indicated by Δy of 46 m. The discretization needed to simulate canal flow is 7.77 km.

The values of $\exp(-\sqrt{0.5P_r}/P_m)$ in the table are closer to 1.0 when the period T_p is long. This indicates that the sediment layer is relatively pervious under such conditions and does not insulate the aquifer from disturbances in the canal. The same sediment layer can insulate the aquifer if the period of the disturbance in the canal is short.

SUMMARY AND CONCLUSIONS

St. Venant equations with the diffusion flow assumption coupled with 2D groundwater flow equations and sediment resistance equations were solved to obtain analytical solutions for small amplitude water-level disturbances. The analytical solution is valid when $P_r << 1$ and when the sediment layer δ is relatively thin. Both of these conditions are satisfied for most applications.

The results show that the solution depends on three-dimensionless parameter groups P_d, $P_b/\sqrt{P_r}$ and $P_m/\sqrt{0.5P_r}$ that can be computed using canal properties, aquifer properties, sediment properties, and the periods of disturbance. The results show that the amplitude of the water level in the canal decays faster, and the speed of disturbance propagation becomes lower, when there is stream-aquifer interaction. The interaction effects are less significant when the period of the disturbance is small, the width of the canal is large, and the aquifer transmissivity is small.

The analytical solution of the problem can be used to determine conditions under which the stream-aquifer interaction is not important when studying the transient flow behavior in canals. In the case of relatively deep canals ($P_d > 0.5$), for example, this occurs approximately when $\chi > 10$, according to Figs. 2 and 3. The figures can be used to understand the domain for which the interaction is negligible. This domain is the area for which the solution $\hat{\lambda}$ does not change with χ. A sediment layer in the canal can also prevent stream-aquifer interaction by insulating the aquifer. The condition for more than 95% cutoff of the stream aquifer interaction is given by $P_m/\sqrt{0.5P_r} < 1/3$.

The analytical solutions were tested against a number of test simulations using the MODFLOW model and the HSE. One of the test problems was very similar to an example of Pinder and Sauer (1971). The results of all simulations show that the analytical and numerical model solutions agree closely. The differences can be due to numerical errors and the difficulty of setting up a numerical model to match exactly the conditions in the analytical solution.

A number of practical applications were used to demonstrate the usefulness of the analytical solution. In two such applications, stream-aquifer interaction was shown to have a significant affect on the decay behavior of water levels in the L31N and Snapper Creek Canals in South Florida. Results show that the disturbances in the canal do not travel far into the aquifer.

The results of the study can be used to understand and quantify stream-aquifer interaction, influence of the sediment layer, and the discretization needed for numerical simulations. Using methods of error analysis (Lal 2000), it is possible to show that relatively small spatial discretizations are needed perpendicular to the canal to model the stream-aquifer interaction accurately.

ACKNOWLEDGMENTS

The writer wishes to thank Todd Tisdale, Joel Van-Arman, Victor Kelson, and Steven Krupa of the SFWMD for reviewing the paper; Mark Belnap for writing the HSE code in C++; and Jayantha Obeysekera, Randy van Zee, and others in the Hydrologic System Modeling Division for valuable comments.

REFERENCES

Bouwer, H. (1965). "Theoretical aspects of seepage from open channels." *J. Hydr. Div.*, ASCE, 91(3), 37–59.

Chin, D. (1990). "A method to estimate canal leakage into the Biscayne Aquifer, Dade County, Florida." *Water Resour. Investigations Rep. No. 90-4135*, U.S. Geological Survey, Tallahassee, Fla.

Chin, D. A. (1991). "Leakage of clogged channels that partially penetrate surficial aquifers." *J. Hydr. Engrg.*, ASCE, 117(4), 467–488.

Dillon, P. J., and Liggett, J. A. (1983). "An ephemeral stream-aquifer interaction model." *Water Resour. Res.*, 19(3), 621–626.

Fish, J. E., and Stewart, M. (1991). "Hydrogeology of the surficial aquifer system, Dade County, Florida." *USGS Water Resour. Investigation Rep. 90-4108*, Tallahassee, Fla., 16–26.

Genereux, D., and Guardiario, J. (1998). "A canal drawdown experiment for determination of aquifer parameters." *J. Hydrologic Engrg.*, ASCE, 3(4), 294–302.

Jorgensen, D. G., Signor, D. C., and Imes, J. L. (1989). "Accounting for intercell flow in models with emphasis on water table recharge and stream-aquifer interaction." *Water Resour. Res.*, 25(4), 669–676.

Lal, A. M. W. (1998a). "Performance comparison of overland flow algorithms." *J. Hydr. Engrg.*, ASCE, 124(4), 342–349.

Lal, A. M. W. (1998b). "Weighted implicit finite-volume model for overland flow." *J. Hydr. Engrg.*, ASCE, 124(9), 941–950.

Lal, A. M. W., Belnap, M., and Van Zee, R. (1998). ''Simulation of overland and ground-water flow in the Everglades National Park.'' *Proc., Int. Water Resour. Engrg. Conf.*, ASCE, Reston, Va., 610–615.
Lal, A. M. W. (2000). ''Numerical errors in groundwater and overland flow models.'' *Water Resour. Res.*, 36(5), 1237–1247.
McDonald, M., and Harbaugh, A. (1988). ''A modular three-dimensional finite-difference ground-water model.'' *U.S. Geological Survey Techniques of Water Resour. Investigations Rep.*, Book 6, Chapter A1, Government Printing Office, Washington, D.C., 576.
Moench, A. F., and Barlow, P. M. (2000). ''Aquifer response to stream-stage and recharge variations. I. Analytical step-response functions.'' *J. Hydrology*, 230(3-4), 192–210.
Morel-Seytoux, H. J. (1975). ''Numerical model for flow in a stream aquifer system.'' *Hydrology Paper 74*, Colorado State University, Fort Collins, Colo.
Pinder, G. F., and Sauer, S. P. (1971). ''Numerical simulation of flood wave modification due to bank storage effects.'' *Water Resour. Res.*, 7(2), 63–70.
Ponce, V. M., Li, R.-M., Simons, D. B. (1978). ''Applicability of kinematic and diffusion models.'' *J. Hydr. Div.*, ASCE, 104(3), 353–361.
Samuels, P. G., and Skells, C. P. (1990). ''Stability limits for Preissman's scheme.'' *J. Hydr. Div.*, ASCE, 116(8), 997–1012.
Schaffranek, R. W. (1987). ''Flow model for open-channel reach or network.'' *USGS Professional Paper 1384*, U.S. Geological Survey, Government Printing Office, Washington, D.C., 11.
South Florida Water Management District (SFWMD). (1999). *A primer to the South Florida water management model (SFWMM) Version 3.5*. West Palm Beach, Fla.
Swain, E. D., and Wexler, E. J. (1996). ''Chapter A6: A coupled surface-water and ground-water flow model (MODBRANCH) for simulation of stream-aquifer interaction.'' *Techniques of water resources investigations of the USGS*, U.S. Geological Survey, Government Printing Office, Washington, D.C.
U.S. Army Corps of Engineers (USACE). (1996). *One-dimensional unsteady flow through a full network of open channels*. Hydrologic Engineering Center, UNET, Davis, Calif.
Walton, R., Wexler, E. J., and Chapman, R. S. (1999). ''An integrated groundwater–open channel flow model.'' *Tech. Rep.*, WEST Consultants, Bellevue, Wash.
Wolfram, S. (1996). *The mathematica book*, 3rd Ed., Cambridge University, London.
Wylie, C. R. (1979). *Differential equations*, McGraw-Hill, New York.
Zitta, V. L., and Wiggert, J. M. (1971). ''Flood routing in channels with bank storage.'' *Water Resour. Res.*, 7(5), 1341–1345.
Zlotnik, V. A., and Huang, H. (1999). ''Effects of shallow penetration and structural streamed sediments on aquifer response to stream stage fluctuations (Analytical model).'' *Ground Water*, 37(4), 599–605.

NOTATION

The following symbols are used in this paper:

B = width of canal (m);
f = complex constant used to describe analytical solution = $f_1 + f_2 I$, for some problems, f_1 is a time decay constant and f_2 is a frequency;
$\hat{f}$ = variable f made dimensionless using f/f_r;
f_r = a disturbing frequency of system;
H = water head (m);
h = water depth in canal (m);
h' = perturbed values of water depth in canal (m);
h_0 = steady-state water depth in canal (m);
k_m = conductivity of the sediment layer (m/s);
m, n = constants used in flow roughness equation;
$P_r, P_d, P_b, \ldots$ = dimensionless parameters used to describe problem;
q = discharge per unit width in canal (m^2/s);
s_c = storage coefficient;
S_f = friction slope;
S_0 = bed slope;
T_c = a linearized flow resistance for the canal (m^2/s)
T_g = transmissivity of aquifer (m^2/s);
T_m = sediment resistance, defined as $T_m = 0.5Bk_m$ (m^2/s);
T_p = period of water level fluctuation (s);
t = time (s); and
x, y = distances along horizontal coordinate axes (m).